Supporting Information

Structurally characterized Ni(II) complex exhibiting potent anti-Candida activity: Biomolecular interaction mechanism and in silico ADMET insights

Alipe Saha*[a], Ribhu Maity*[b], Gurupada Dhara[b], Paula Brandao[c], Satyajit Pattanayak[b], Tithi Maity[d], Keka Sarkar**[a] and Bidhan Chandra Samanta**[b]

[a]*Department of Microbiology, University of Kalyani, West Bengal, India*

[b]*Department of Chemistry, Mugberia Gangadhar Mahavidyalaya, Bhupatinagar, Purba Medinipur, West Bengal, India.*

[c]*Departamento de Química, CICECO, Universidade de Aveiro, 3810-193 Aveiro, Portugal*

[d]*Department of Chemistry, Prabhat Kumar College, Purba Medinipur, Contai, West Bengal, India*

* First authors: Alipe Saha and Ribhu Maity (Equal contribution)

Corresponding authors:** bidhansamanta@yahoo.in **(BCS);** keka@klyuniv.ac.in **(KS)**

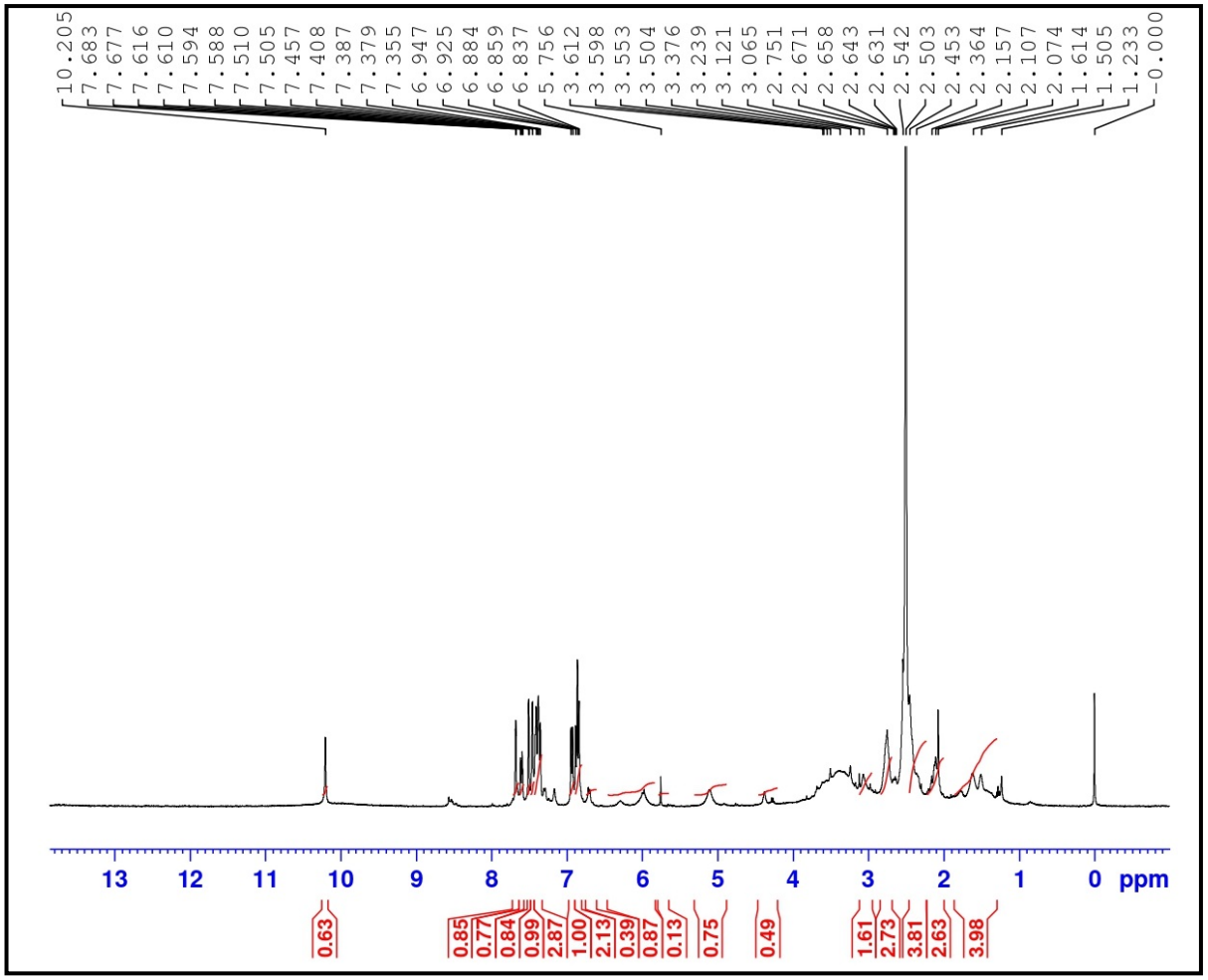

Fig. S1 ^{1}H NMR spectrum of the ligand

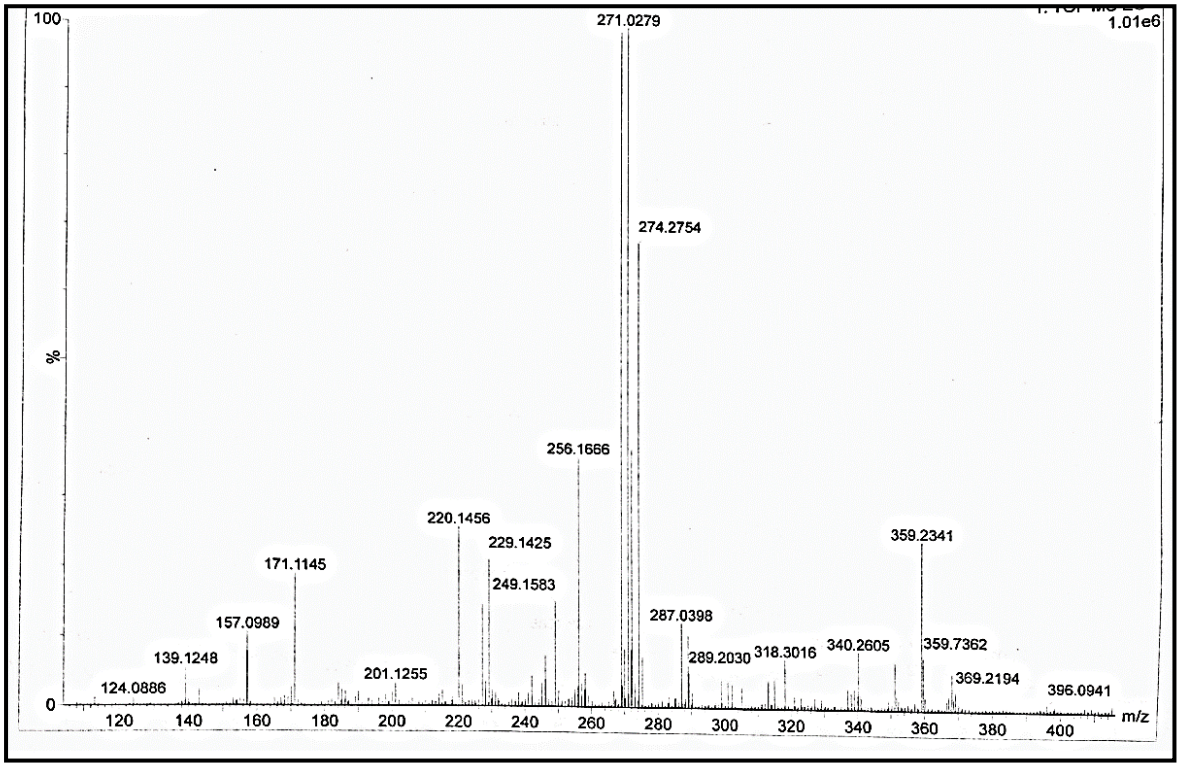

Fig. S2 Mass spectrum of the ligand

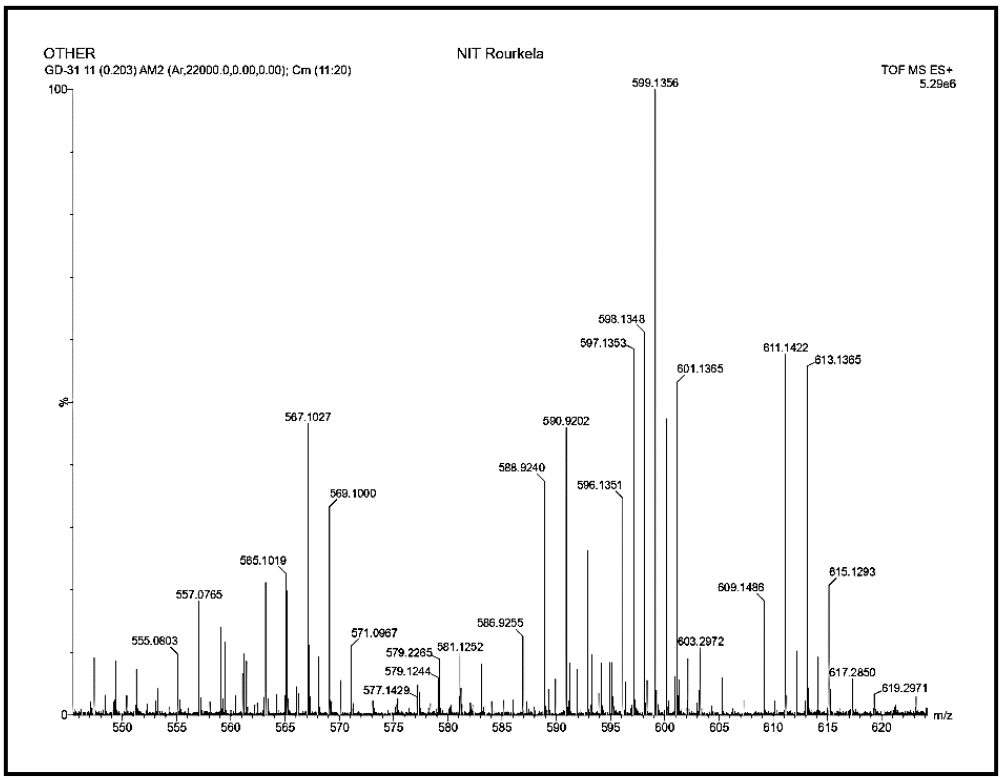

Fig. S3 Mass spectrum of the complex

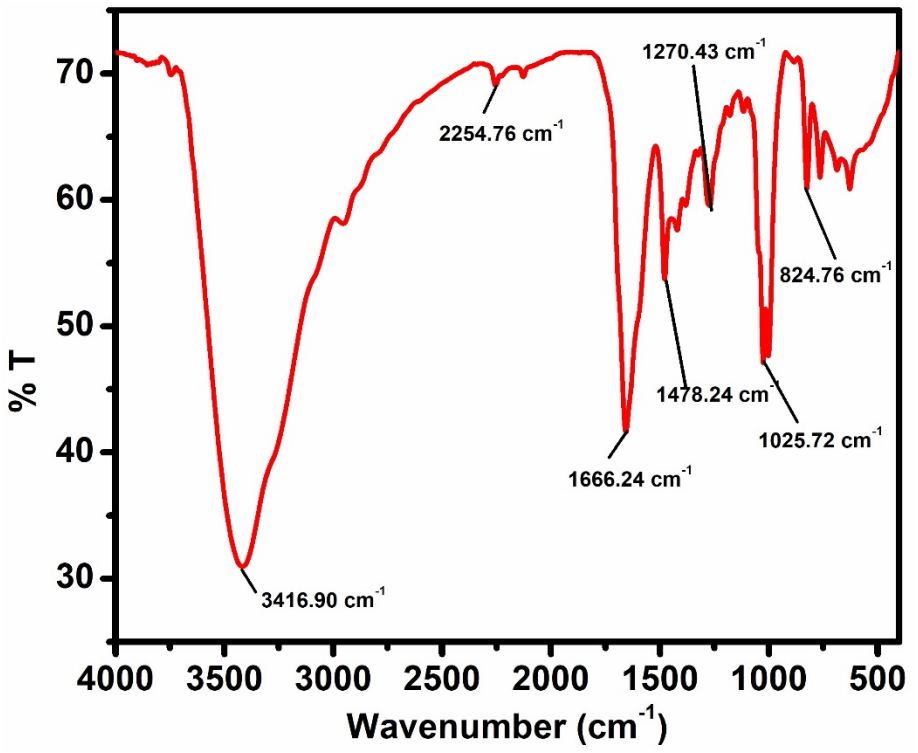

Fig. S4 FTIR spectrum of the ligand

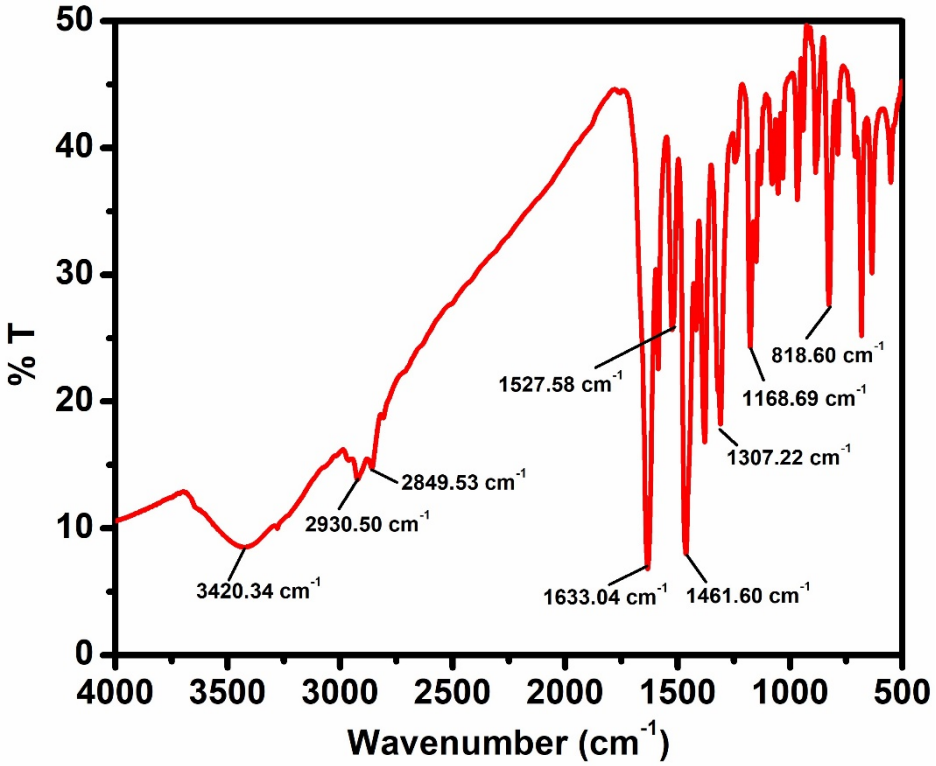

Fig. S5 FTIR spectrum of the complex

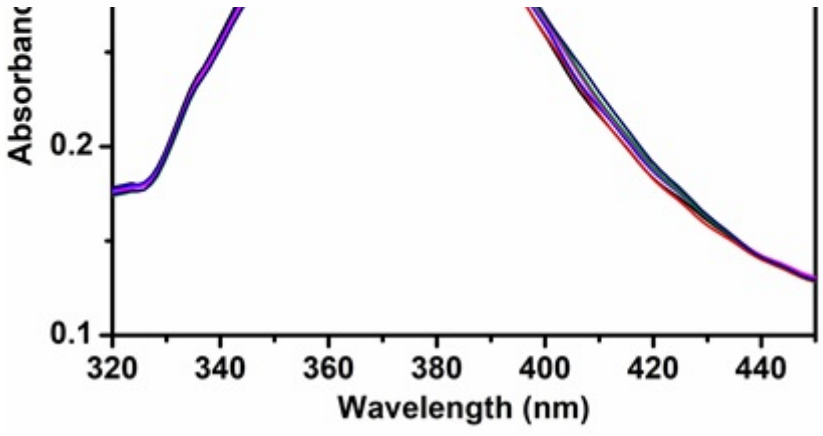

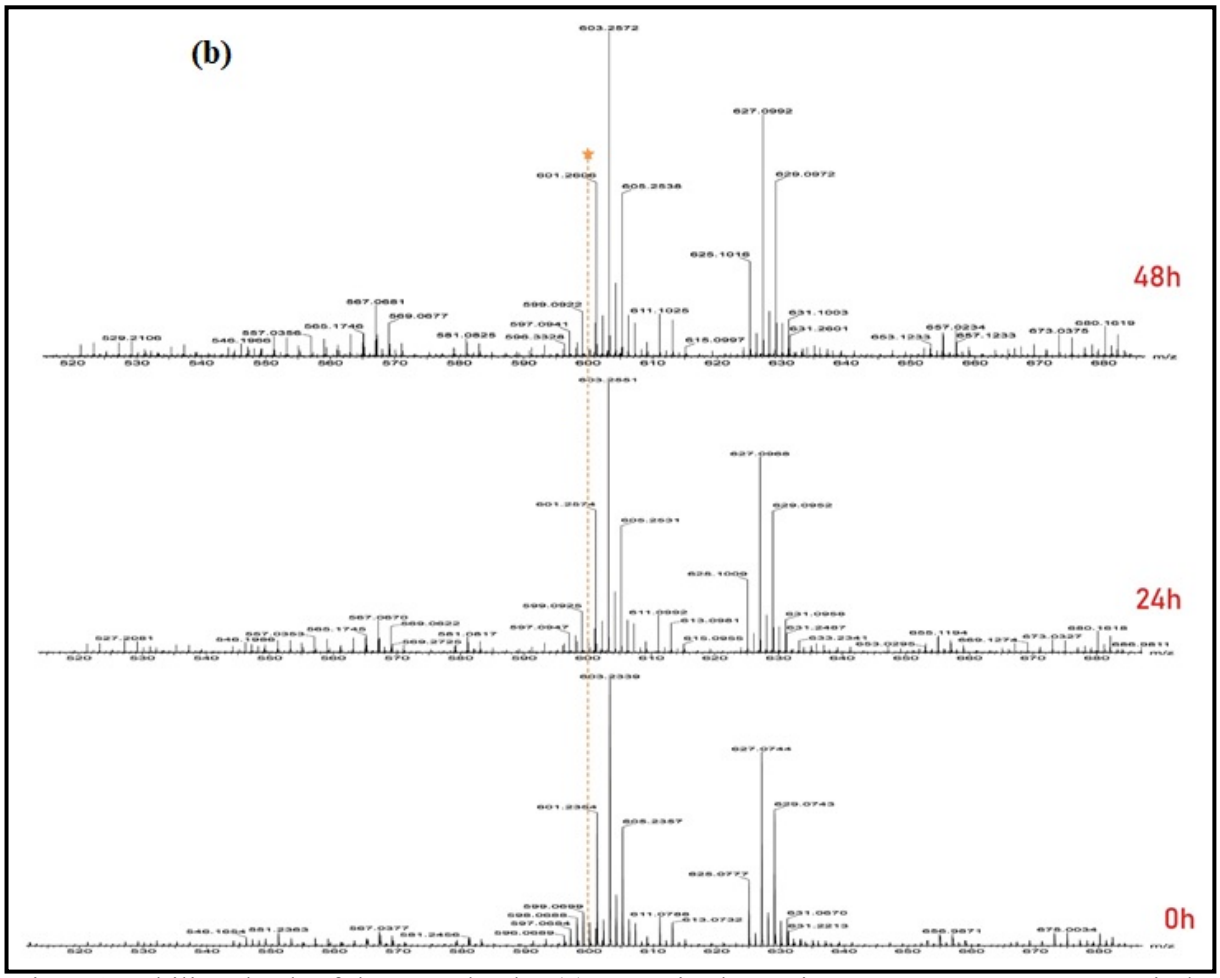

Fig. S6 Stability check of the complex by (a) UV-Vis absorption spectroscopy over a period of six days (b) Time-dependent ESI-MS taken at 0h, 24h and 48h.

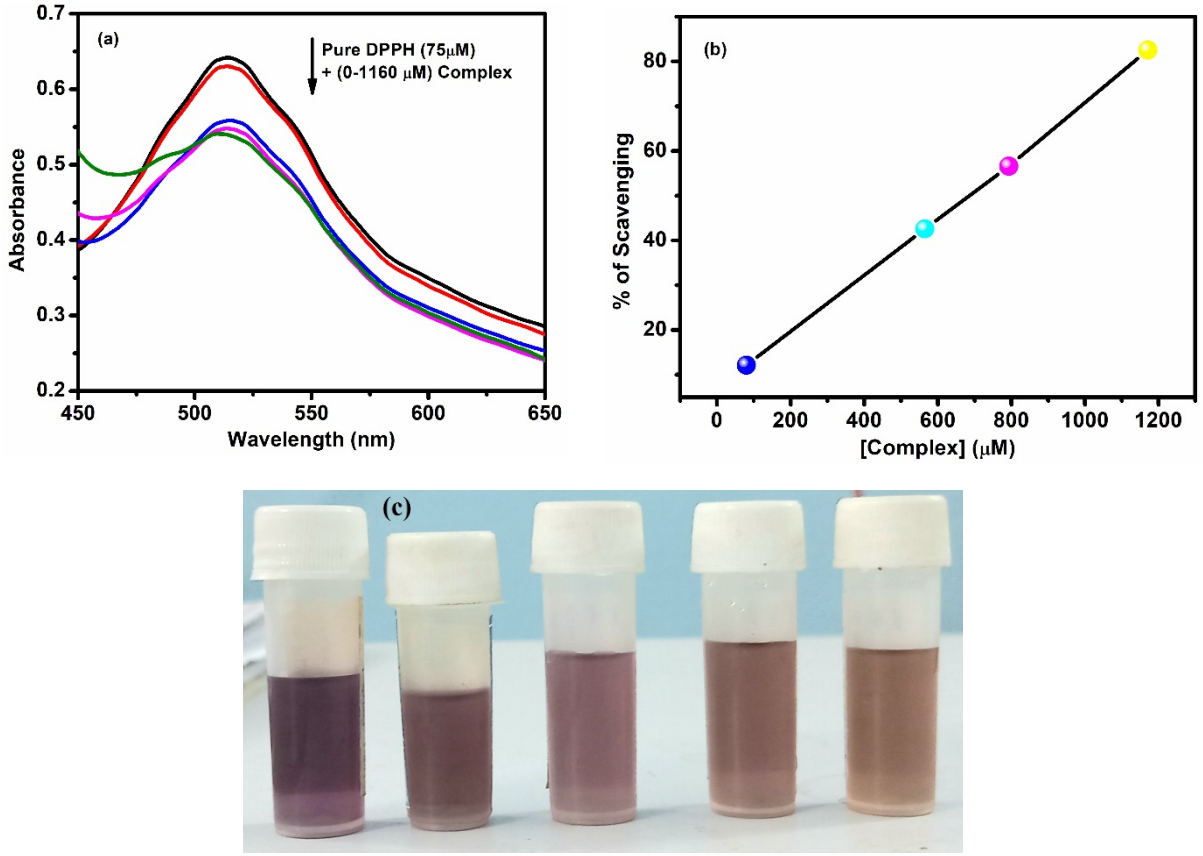

Fig. S7 (a) Absorbance changes of DPPH with gradual addition of the complex (b) IC_{50} graph (c) Colour changes of pure DPPH solution with incremental addition of the complex

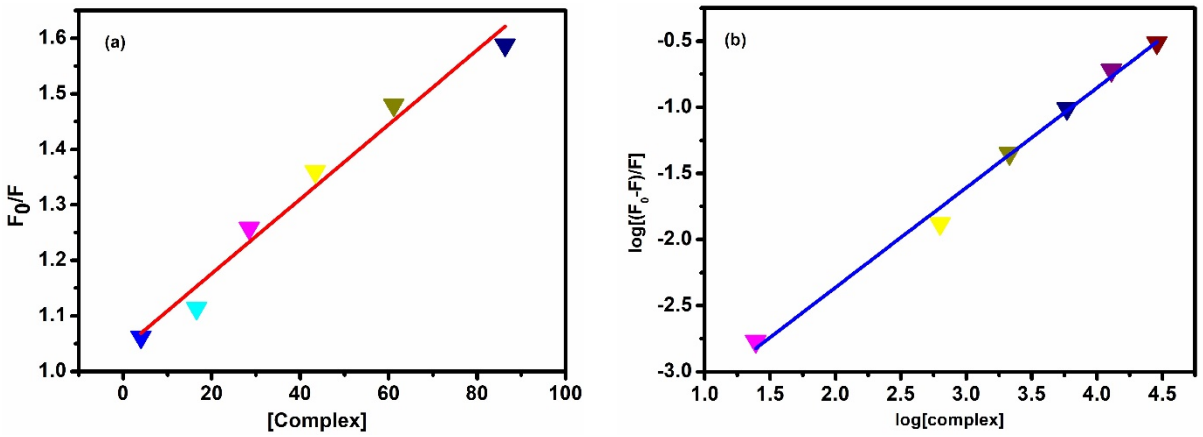

Fig. S8 (a) Stern–Volmer plot and (b) Scatchard plot for binding interactions of the complex with DNA-EB system

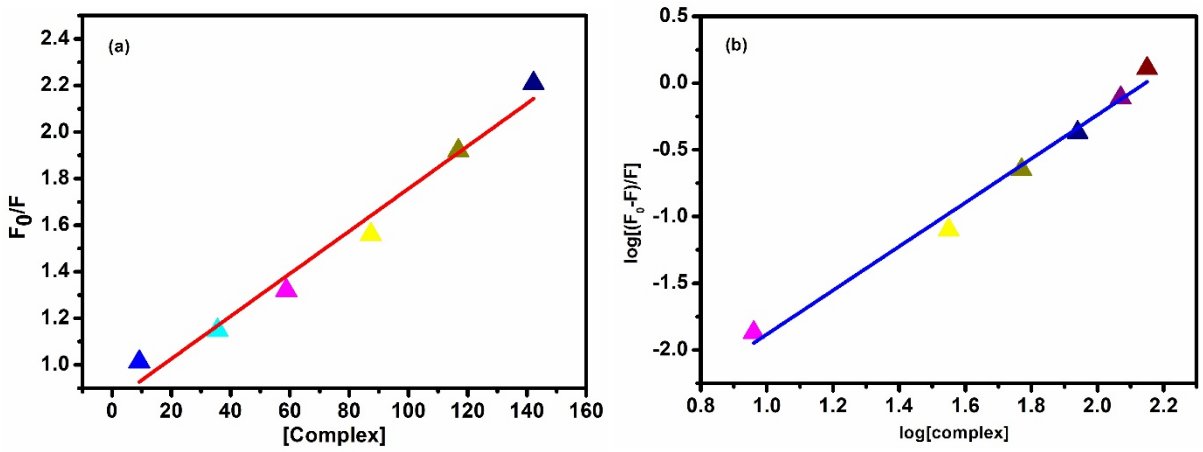

Fig. S9 (a) Stern–Volmer plot and (b) Scatchard plot for binding interactions of the complex with DNA-Hoechst system

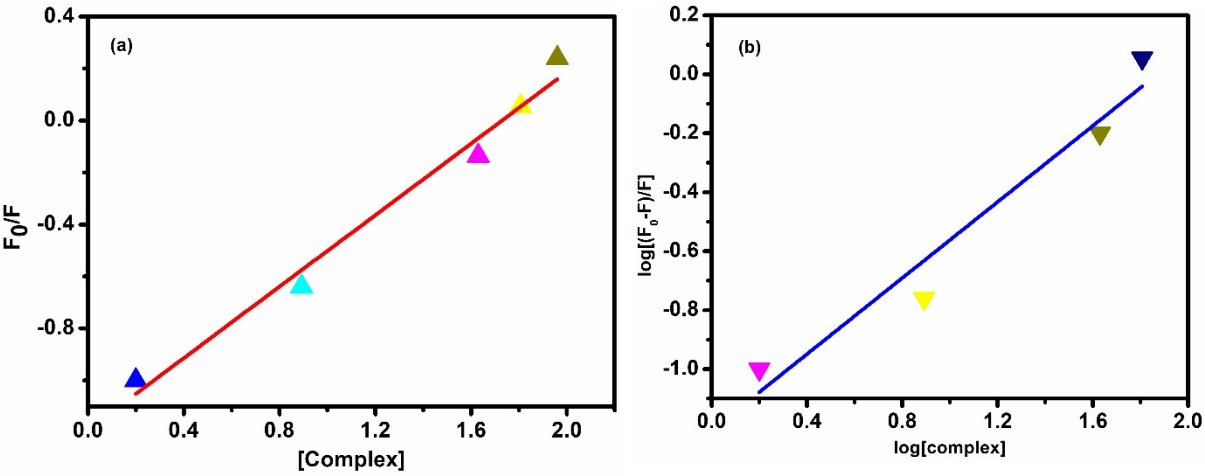

Fig. S10 (a) Stern–Volmer plot and (b) Scatchard plot for binding interactions of the complex with BSA protein

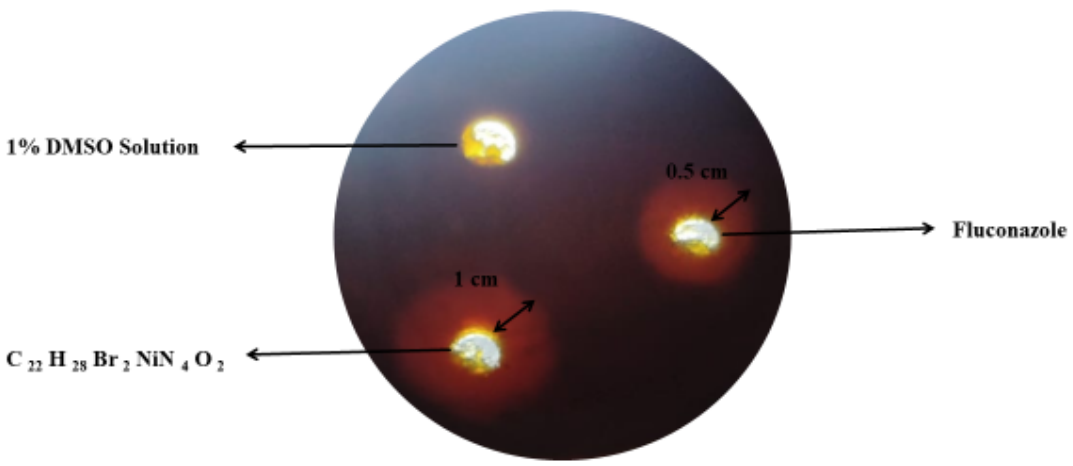

Fig. S11 Agar cup assay with 3 conditions: I. Complex II. 1% DMSO Solution, III. Fluconazole

Table S1 Relevant bond distances (Å) and angles (º) for the complex $[Ni(L)_2]$

Bond lenghts		**Bond angles**	
Ni(1)-O(1)	2.0321(17)	O(1)-Ni(1)-O(1i)	180.00(8)
Ni(1)-O(1i)	2.0321(17)	O(1)-Ni(1)-N(1)	87.08(7)
Ni(1)-N(1)	2.059(2)	O(1)-Ni(1)-N(1i)	92.92(7)
Ni(2)-N(1i)	2.059(2)	O(1)-Ni(1)-N(2)	87.96(6)
Ni(2)-N(2)	2.204(2)	O(1)-Ni(1)-N(2i)	92.04(8)
Ni(2)-N(2i)	2.204(2)	N(1)-Ni(1)-N(2)	82.44(8)
Br(1)-C(4)	1.899(3)	N(1i)-Ni(1)-N(2)	97.56(8)

Table S2 PrankWeb identified rank 1 pocket details

Parameter	**Details**
Rank	**1**
Score	**70.54**
Probability	**0.990**
Number of residues	**56**
Pocket center	**(-42.2893, -12.9357, 23.8963)**

Residues	**A_105, A_117, A_118, A_122, A_126, A_131, A_132, A_139, A_143, A_146, A_150, A_200, A_204, A_228, A_230, A_233, A_300, A_303, A_304, A_305, A_307, A_308, A_309, A_311, A_312, A_315, A_370, A_376, A_377, A_378, A_379, A_380, A_381, A_401, A_462, A_463, A_464, A_468, A_469, A_470, A_471, A_472, A_475, A_476, A_479, A_480, A_505, A_507, A_508, A_509, A_61, A_64, A_65, A_87, A_88, A_90**
Average conservation score	**1.099**
Ligand-bound/free PDB structures	**Prefilled AHoJ query URL (5V5Z A LEU 376)**

Table S3 Docking results with different parameters and software.

Compound	Protein Target	Docking Tool	Docking Type	Binding Affinity (kcal/mol)
Complex	**CYP51**	**MzDock**	**Blind docking**	**-9.5**
Complex	**CYP51**	**MzDock**	**Specific docking**	**-9.5**
Complex	**CYP51**	**CB-Dock2**	**Redocking**	**-10.5**
Fluconazole	**CYP51**	**CB-Dock2**	**Redocking**	**-7.4**

Table S4 Comparative results of docking through CB-Dock2 of Fluconazole and complex

Parameter	Fluconazole	Complex
Vina Score (kcal/mol)	**-7.3**	**-10.5**
Cavity Volume (Å³)	**5073**	**5073**
Center (x, y, z)	**(-38, -14, 25)**	**(-38, -14, 25)**
Docking Size (x, y, z)	**(35, 26, 20)**	**(35, 21, 21)**

Contact Residues	**PHE105, TYR118, LEU121, THR122, PHE126, ILE131, TYR132, LEU139, GLN142, LYS143, ALA146, LYS147, ALA149, LEU150, ALA200, LEU204, PHE228, PHE233, LEU276, LEU300, GLY303, ILE304, LEU305, MET306, GLY307, GLY308, GLN309, HIS310, THR311, SER312, LEU376, ILE379, ARG381, PRO462, PHE463, GLY464, GLY465, HIS468, ARG469, CYS470, ILE471, GLY472, GLU473, PHE475, ALA476, GLN479, MET508, VAL509**	**PHE105, TYR118, LEU121, THR122, PHE126, ILE131, TYR132, LEU139, GLN142, LYS143, PHE228, PHE233, LEU300, GLY303, ILE304, GLY307, GLY308, THR311, MET374, PRO375, LEU376, ILE379, ARG381, LEU461, PRO462, PHE463, GLY464, GLY465, HIS468, ARG469, CYS470, ILE471, GLY472, PHE475, MET508, VAL509**